Centering the Trajectory in Radial TrueFISP Imaging: Comparing Gradient Delay Modeling and Phase Correction Strategies

K. J. Barkauskas[1], C. M. Hillenbrand[2], J. L. Duerk[2]

[1]Biomedical Engineering, Case Western Reserve University, Cleveland, Ohio, United States, [2]Radiology, University Hospitals of Cleveland, Cleveland, Ohio, United States

Introduction: Streak artifacts in radial MR imaging result from a variety of sources including trajectories that are not centered at the K-space origin. One post-hoc compensation strategy is to measure the K-space trajectory [1], which can be used to properly map each sample during gridding to its "true" location within a Cartesian K-space grid. Alternatively, gradient delay modeling [2] and image domain phase correction [3] are more flexible alternatives that attempt to correct the data prior to gridding. Both methods correct for trajectory errors in the logical reference frame, which makes them independent of orientation and relatively insensitive to sequence parameters. Gradient delay modeling assumes the variation in echo timing across projections can be approximated by small time delays between each physical waveform that is sourced from its respective gradient power amplifier. Recently, a model independent correction was proposed for PROPELLER acquisitions, (which combine both radial and rectilinear trajectory elements). The "blade" alignment process of PROPELLER removes image domain phase which arises from errors in K-space timing without regard for the true source of the error. Hence, it may provide an effective compensation strategy for gradient delays, trajectory errors and other potential sources of errors in conventional radial imaging. This work determines which method -- PROPELLER-based phase correction or gradient delay modeling -- achieves the best artifact suppression for Radial TrueFISP imaging in resolution phantom, volunteer and clinical imaging trials.

Materials and Methods: A Radial TrueFISP sequence with gradient lobes that can be adjusted to account for gradient delays and ensure echo centering within the sampling window was developed for a 1.5T Siemens Sonata imager (Siemens Medical Solutions, Erlangen Germany). The relevant imaging parameters are: FOV 300mm, Thickness 5mm, TE/TR 3.7/7.4ms, Flip angle 70°, Ns 256, Np 128 through 180°, BW 1000Hz/pixel, 300 dummy cycles prior to the first imaging view. Images were reconstructed offline using 3x3 Kaiser-Bessel kernel convolution gridding scheme with Ram-Lak density compensation [4]. Echo shifts were determined by the Ahn method in the frequency domain [5]. In a separate experiment, physical gradient delays ([GDx GDy GDz] = [1.22 1.69 1.51], μs) were estimated via a routine based on the work of Peters [2] and written in Matlab (The MathWorks, Nattick, MA). A transverse slice was acquired with and without gradient delay correction using the above estimates. Both data sets were gridded with and without PROPELLER-based phase correction, in which the correction map is obtained from K-space projections windowed by a pyramid function [3]. Images of a resolution phantom and the head of an asymptomatic volunteer were obtained. In an ROI adjacent to each object, mean signal amplitude was computed for comparison of background residual streak artifact.

Results: Figure 1 shows echo shifts as a function of projection angle for the resolution phantom. Note that phase correction, unlike gradient delay correction, reduces the echo shift variation across the views to near zero. Figure 2 shows phantom magnitude images after reconstruction. Note that the streak and inhomogeneous amplitude response of the uncorrected data set (Fig. 2a) is absent in both the gradient delay corrected (Fig. 2b) and phase corrected (Fig. 2c) images. By applying the PROPELLER phase correction to gradient delay corrected projections, some of the residual streak artifact (Fig 2b, arrow) is further reduced (Fig. 2d). Similar results were found when in-vivo human head images were acquired (Fig. 3). Note the slight image distortion (Fig. 3c,d, arrow) after phase correction. In general, either correction scheme reduced the "spray" of signal amplitude outside of the object, where the mean value within an ROI have been reported with their corresponding figure. The correction schemes achieved 40-60% reduction in extraneous signal in the background.

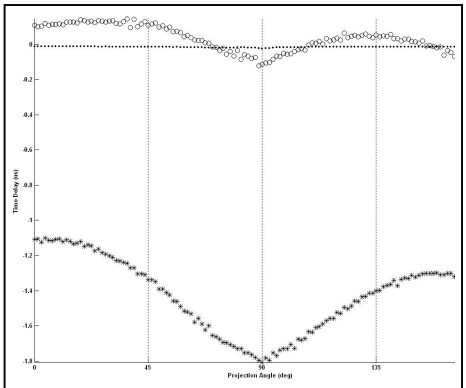

Figure 1: Echo shift (in μs) detected by the Ahn method vs. projection angle after (*) no correction, (o) only gradient delay correction and (•) only PROPELLER-based phase correction.

Discussion: Either the PROPELLER-based phase correction or the gradient delay modeling technique alone can improve the overall image quality, and in some instances the combination of both produces the least artifact. Since the phase correction algorithm proposed for PROPELLER does not assume a degradation model a-priori, it removes nearly all vestiges of echo shift from radial projections. Thus, for example, phase corrected projections of the phantom contain lower levels of error that would otherwise be enhanced by gridding with an assumed ideal trajectory. However, the phase correction process as proposed by Pipe makes no distinction between phase from trajectory error and phase from a spatial distribution of off-resonance. This can lead to severe artifacts in regions, such as the sinuses of the head, that contain more off-resonance than we demonstrate in this work. Despite the potential problem with off-resonance and based upon simplicity, flexibility and remarkable results, we conclude that PROPELLER-based phase correction for conventional radial TrueFISP imaging achieves equal if not superior image quality compared to gradient delay modeling alone.

References:
(1) Duyn, JH, et al. JMR 1998. 132:150-153
(2) Peters, DC, et al. MRM 2003. 50:1-6
(3) Pipe, JG. MRM 1999. 42: 963-969
(4) Dale, BM, et al. IEEE Trans Med Imag 2001. 20:207-217
(5) Ahn, CB and Cho, ZH. IEEE Trans Med Imag 1987.6:32-36

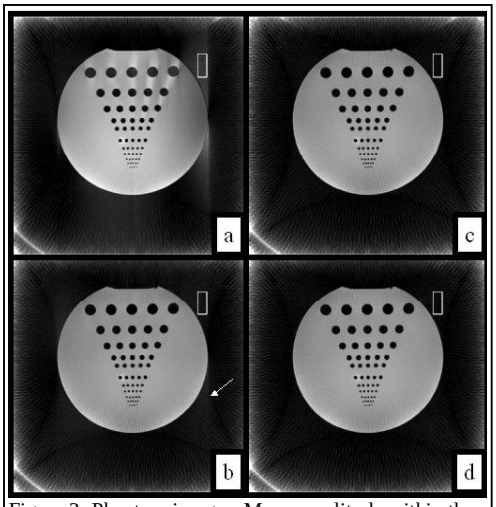

Figure 2: Phantom images. Mean amplitude within the rectangular ROI is in parentheses for: (a) no correction (46.0), (b) only gradient delay correction (22.7), (c) only PROPELLER-based phase correction (22.8), and (d) both gradient delay and phase correction (27.7).

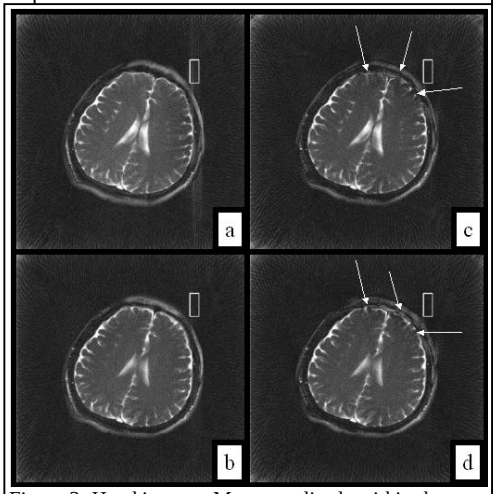

Figure 3: Head images. Mean amplitude within the rectangular ROI is in parentheses for: (a) no correction (18.1), (b) only gradient delay correction (10.9), (c) only PROPELLER-based phase correction (7.19), and (d) both gradient delay and phase correction (7.7).